Ocean Engineering 266 (2022) 113016

Contents lists available at ScienceDirect

Ocean Engineering

journal homepage: www.elsevier.com/locate/oceaneng

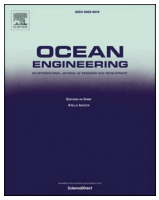

Novel reliability method validation for offshore structural dynamic response

Oleg Gaidai [a], Yihan Xing [b,*]

[a] Shanghai Ocean University, Shanghai, China
[b] University of Stavanger, Stavanger, Norway

ARTICLE INFO

Keywords:
Reliability
Failure probability
Dynamic system
Fossil energy

ABSTRACT

The paper validates novel structural reliability Gaidai-Fu-Xing (GFX) method, particularly suitable for multi-dimensional structural responses, versus well established bivariate statistical method, that is known to accurately predict two-dimensional system extreme response levels. Classic reliability methods, dealing with time series do not have an advantage of dealing easily with system high dimensionality and cross-correlation between different dimensions. An operating Jacket located in the Bohai bay was taken as an example to demonstrate the proposed methodology. Novel state of art bimodal extrapolation technique was applied to predict system reliability with five years return period, which is of practical importance for design of fixed offshore structures.

Unlike other reliability methods the new method does not require to re-start simulation each time system fails, in case of numerical simulation. In case of measured structural response, an accurate prediction of system failure probability is also possible as illustrated in this study.

Jacket offshore platform subjected to large environmental wave loads, thus structural stresses in different structural critical locations were chosen as an example for this reliability study. The method proposed in this paper opens up the possibility to predict simply and efficiently failure probability for nonlinear multi-dimensional dynamic system as a whole.

1. Introduction

For Bohai sea location see Fig. 1. Due to significant increase of scientific and economic interest, especially offshore oil and gas and marine engineering industry. Bohai sea in situ wave characteristics are the key input for both offshore structural and reliability study, see (Lv et al., 2014), (Wang et al., 2012) for Bohai bay local wave data, and DNV standards (DNV-RP-H103, 2011), (DNV-RP-C205, 2010) for the engineering guidance. It is challenging to estimate structural system reliability by using classic engineering reliability methods (Norwegian Meteorological Institute)- (Melchers, 1999), (Thoft-Christensen and Murotsu, 1986), (Sharma and Dean, 1981; Adcock and Draper, 2015; Zhao and Ono, 1999). The latter is usually due to high number of degrees of system freedom and random variables governing dynamic system. Reliability of a complex structural systems can be straightforwardly estimated either by having enough measurements or by direct numerical Monte Carlo simulations, (Naess et al., 2009), (Naess et al., 2012), (Xing et al., 2022; Gaidai et al., 2022a, 2022b; Sun et al., 2022b; Xu et al., 2022a). However, experimental and computational often are unaffordable for many complex engineering dynamic systems. Authors have introduced novel reliability method for structural systems aiming at reduction of either measurement or numerical computational costs.

This paper studies Jacket stress structural responses, subject to environmental drag-dominated loads, acting on the support structure in rough seas.

This paper advocates a novel Monte Carlo (MC) based statistical approach, naturally being able to tackle inherent nonlinear effects. Due to certain correlation between stresses in different structural support members - application of the multivariate extreme value theory is of practical importance.

For practical engineering use of the suggested methodology, see Fig. 2, where on the flow chart input side are the in situ environmental conditions, while on the output side is the dynamic system target failure probability. There is a great need in new statistical methods to be able to efficiently utilize limited non-stationary data set, then estimate probability of extreme events. The novel approach advocated in this paper has been validated by comparison with method previously benchmarked in various applications, (Gaidai et al., 2022c, 2022d; Xu et al., 2022b).

* Corresponding author.
E-mail address: yihan.xing@uis.no (Y. Xing).

https://doi.org/10.1016/j.oceaneng.2022.113016
Received 8 September 2022; Received in revised form 23 October 2022; Accepted 25 October 2022
Available online 28 November 2022

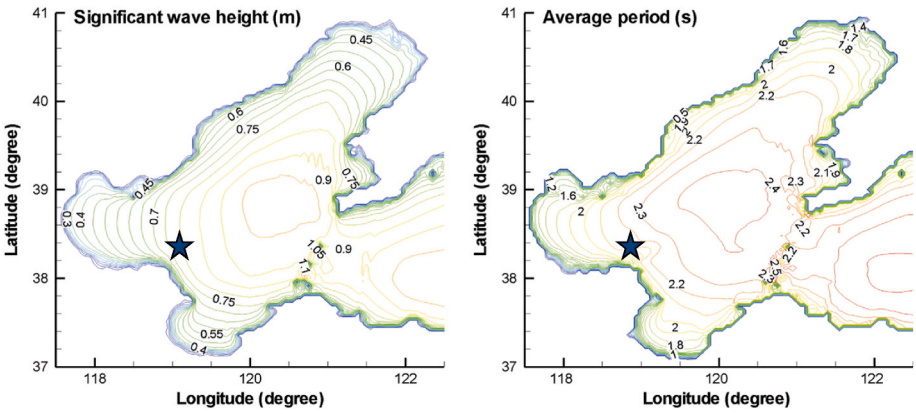

Fig. 1. Annually averaged spatial distribution of wave height and period in Bohai bay (Lv et al., 2014), stars indicates Jacket location.

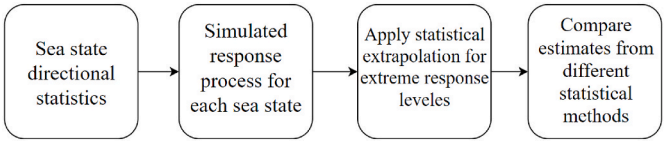

Fig. 2. Long term statistical analysis flow chart.

Note that novel Gaidai-Fu-Xing (GFX) method (Gaidai et al., 2022) is MDOF (multi degree of freedom), while ACER2D (Xu et al., 2022a) is only limited to 2DOF (two dimensions), moreover ACER2D does not provide confidence intervals, while new GFX method can. The main objective of this paper is to coin novel improved method for assessment of extreme response, with special emphasis on whipping.

2. Method

Consider an MDOF (multi-degree of freedom) jointly stationary structural response. The MDOF structural response vector process $\boldsymbol{R}(t) = (X(t), Y(t), Z(t), \ldots)$ is measured and/or simulated over a sufficiently long time interval $(0, T)$. Unidimensional global maxima over the entire time span $(0, T)$ are denoted as $X_T^{\max} = \max_{0\le t\le T} X(t)$, $Y_T^{\max} = \max_{0\le t\le T} Y(t)$, $Z_T^{\max} = \max_{0\le t\le T} Z(t), \ldots$.By sufficiently long time T one primarily means a large value of T with respect to the dynamic system auto-correlation time.

Let $X_1, \ldots, X_{N_X}$ be consequent in time local maxima of the process $X(t)$ at monotonously increasing discrete time instants $t_1^X < \ldots < t_{N_X}^X$ in $(0, T)$. The analogous definition follows for other MDOF response components $Y(t), Z(t), \ldots$ with $Y_1, \ldots, Y_{N_Y}$; $Z_1, \ldots, Z_{N_Z}$ and so on. For simplicity, all $\boldsymbol{R}(t)$ components, and therefore its maxima are assumed to be non-negative. The aim is to estimate system failure probability

$$1 - P = \text{Prob}\left(X_T^{\max} > \eta_X \cup Y_T^{\max} > \eta_Y \cup Z_T^{\max} > \eta_Z \cup \ldots\right) \tag{1}$$

with

$$P = \iiint_{(0,0,0,\ldots)}^{(\eta_X,\eta_Y,\eta_Z,\ldots)} p_{X_T^{\max},\, Y_T^{\max},\, Z_T^{\max},\,\ldots}\left(X_T^{\max}, Y_T^{\max}, Z_T^{\max}, \ldots\right) dX_T^{\max} dY_{N_Y}^{\max} dZ_{N_z}^{\max} \ldots \tag{2}$$

being the probability of non-exceedance for response components $\eta_X, \eta_Y, \eta_Z, \ldots$ critical values; $\cup$ denotes logical unity operation « or»; and $p_{X_T^{\max},\, Y_T^{\max}, Z_T^{\max},\ldots}$ being joint probability density of the global maxima over the entire time span $(0, T)$.

In practice, however, it is not feasible to estimate the latter joint probability distribution directly $p_{X_T^{\max},\, Y_T^{\max}, Z_T^{\max},\ldots}$ due to its high dimensionality and available data set limitations. In other words, the time instant when either $X(t)$ exceeds η_X, or $Y(t)$ exceeds η_Y, or $Z(t)$ exceeds η_Z, and so on, the system being regarded as immediately failed. Fixed failure levels $\eta_X, \eta_Y, \eta_Z, \ldots$ are of course individual for each unidimensional response component of $\boldsymbol{R}(t)$. $X_{N_X}^{\max} = \max\{X_j; j = 1, \ldots, N_X\} = X_T^{\max}$, $Y_{N_Y}^{\max} = \max\{Y_j; j = 1, \ldots, N_Y\} = Y_T^{\max}$, $Z_{N_z}^{\max} = \max\{Z_j; j = 1, \ldots, N_Z\} = Z_T^{\max}$, and so on.

Next, the local maxima time instants $[t_1^X < \ldots < t_{N_X}^X;\ t_1^Y < \ldots < t_{N_Y}^Y;\ t_1^Z < \ldots < t_{N_Z}^Z]$ in monotonously non-decreasing order are sorted into one single merged time vector $t_1 \le \ldots \le t_N$.Note that $t_N = \max\{t_{N_X}^X, t_{N_Y}^Y, t_{N_Z}^Z, \ldots\}$, $N = N_X + N_Y + N_Z + \ldots$. In this case t_j represents local maxima of one of MDOF stationary system response components either $X(t)$ or $Y(t)$, or $Z(t)$ and so on. That means that having $\boldsymbol{R}(t)$ time record, one just needs continuously and simultaneously screen for unidimensional response component local maxima and record its exceedance of MDOF limit vector $(\eta_X, \eta_Y, \eta_Z, \ldots)$ in any of its components $X, Y, Z, \ldots$. The local unidimensional response component maxima are merged into one temporal non-decreasing vector $\vec{R} = (R_1, R_2, \ldots, R_N)$ in accordance with the merged time vector $t_1 \le \ldots \le t_N$. That is to say, each local maxima R_j is the actual encountered local maxima corresponding to either $X(t)$ or $Y(t)$, or $Z(t)$ and so on. Finally, the unified limit vector $(\eta_1, \ldots, \eta_N)$ is introduced with each component η_j is either η_X, η_Y or η_Z and so on, depending on which of $X(t)$ or $Y(t)$, or $Z(t)$ etc., corresponding to the current local maxima with the running index j.

Next, a scaling parameter $0 < \lambda \le 1$ is introduced to artificially simultaneously decrease limit values for all response components, namely the new MDOF limit vector $(\eta_X^\lambda, \eta_Y^\lambda, \eta_z^\lambda, \ldots)$ with $\eta_X^\lambda \equiv \lambda \bullet \eta_X$, $\equiv \lambda \bullet \eta_Y$, $\eta_z^\lambda \equiv \lambda \bullet \eta_Z$, … is introduced. The unified limit vector $(\eta_1^\lambda, \ldots, \eta_N^\lambda)$ is introduced with each component η_j^λ is either η_X^λ, η_Y^λ or η_z^λ and so on. The latter automatically defines probability $P(\lambda)$ as a function of λ, note that $P \equiv P(1)$ from Eq. (1). Non-exceedance probability $P(\lambda)$ can be now estimated as follows:

$$\begin{aligned} P(\lambda) &= \text{Prob}\left\{R_N \le \eta_N^\lambda, \ldots, R_1 \le \eta_1^\lambda\right\} = \text{Prob}\left\{R_N \le \eta_N^\lambda \;\middle|\; R_{N-1} \le \eta_{N-1}^\lambda, \ldots, R_1 \le \eta_1^\lambda\right\} \cdot \text{Prob}\left\{R_{N-1} \le \eta_{N-1}^\lambda, \ldots, R_1 \le \eta_1^\lambda\right\} \\ &= \prod_{j=2}^{N} \text{Prob}\left\{R_j \le \eta_j^\lambda \;\middle|\; R_{j-1} \le \eta_{1j-}^\lambda, \ldots, R_1 \le \eta_1^\lambda\right\} \cdot \text{Prob}\left(R_1 \le \eta_1^\lambda\right) \end{aligned} \tag{3}$$

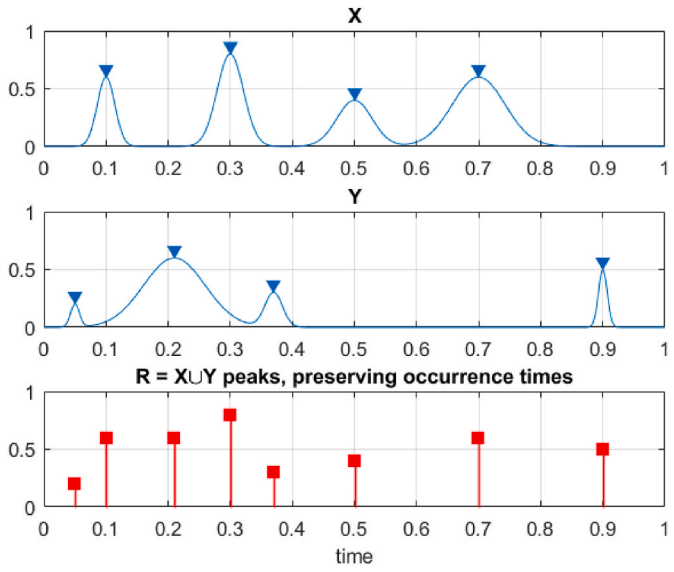

Fig. 3. Illustration on how two exemplary processes X and Y are combined into new synthetic vector $\boldsymbol{R}(t)$.

In practice, dependency between neighbouring R_j is not always negligible; thus, the following one-step (called here conditioning level $k = 1$) memory approximation is introduced:

$$\text{Prob}\left\{R_j \le \eta_j^\lambda \;\middle|\; R_{j-1} \le \eta_{j-1}^\lambda, \ldots, R_1 \le \eta_1^\lambda\right\} \approx \text{Prob}\left\{R_j \le \eta_j^\lambda \;\middle|\; R_{j-1} \le \eta_{j-1}^\lambda\right\} \tag{4}$$

for $2 \le j \le N$ (called here conditioning level $k = 2$). The approximation introduced by Eq. (4) can be further expressed as:

$$\begin{aligned}&\text{Prob}\left\{R_j \le \eta_j^\lambda \;\middle|\; R_{j-1} \le \eta_{j-1}^\lambda, \ldots, R_1 \le \eta_1^\lambda\right\}\\ &\approx \text{Prob}\left\{R_j \le \eta_j^\lambda \;\middle|\; R_{j-1} \le \eta_{j-1}^\lambda, R_{j-2} \le \eta_{j-2}^\lambda\right\}\end{aligned} \tag{5}$$

where $3 \le j \le N$ (will be called conditioning level $k = 3$), and so on. The motivation is to monitor each independent failure that happened locally first in time, thus avoiding cascading local inter-correlated exceedances, (Song, 2017)- (Sumer and Fredsøe, 1997).

Eq. (5) presents subsequent refinements of the statistical independence assumption. The latter type of approximations enables capturing the statistical dependence effect between neighbouring maxima with increased accuracy. Since the original MDOF stationary process $\boldsymbol{R}(t)$ was assumed ergodic and therefore stationary, probability $p_k(\lambda) := \text{Prob}\{R_j > \eta_j^\lambda \;|\; R_{j-1} \le \eta_{j-1}^\lambda, R_{j-k+1} \le \eta_{j-k+1}^\lambda\}$ for $j \ge k$ will be independent of j but only dependent on conditioning level k. Thus non-exceedance probability can be approximated as in the Naess-Gaidai method, (Naess and Moan, 2013), (Rice, 1944), (Sun et al., 2022a)

$$P_k(\lambda) \approx \exp\left(-N \bullet p_k(\lambda)\right), k \ge 1 \tag{6}$$

Note that Eq. (6) follows from Eq. (1) by neglecting $\text{Prob}(R_1 \le \eta_1^\lambda) \approx 1$, as the design failure probability is usually very small. Further, it is assumed $N \gg k$.

Note that Eq. (5) is similar to the well-known mean up-crossing rate equation for the probability of exceedance. There is obvious convergence with respect to the conditioning parameter k:

$$P = \lim_{k\to\infty} P_k(1);\; p(\lambda) = \lim_{k\to\infty} p_k(\lambda) \tag{7}$$

Note that Eq. (6) for $k = 1$ turns into the quite well-known non-exceedance probability relationship with the mean up-crossing rate function

$$P(\lambda) \approx \exp\left(-\nu^+(\lambda)\, T\right);\; \nu^+(\lambda) = \int_0^\infty \zeta p_{R\dot{R}}(\lambda, \zeta) d\zeta \tag{8}$$

where $\nu^+(\lambda)$ is the mean up-crossing rate of the response level λ for the above assembled non-dimensional vector $\boldsymbol{R}(t)$ assembled from scaled MDOF dynamic system response $\left(\frac{X}{\eta_X}, \frac{Y}{\eta_Y}, \frac{Z}{\eta_Z}, \ldots\right)$, see Fig. 3.

In the above, the stationarity assumption has been used. The proposed methodology can also treat the non-stationary case. An illustration of how the methodology can be used to treat non-stationary cases is provided as follows. Consider a scattered diagram of $m = 1, .., M$ environmental states, each short-term environmental state having a probability q_m, so that $\sum_{m=1}^M q_m = 1$. The corresponding long-term equation is then:

$$p_k(\lambda) \equiv \sum_{m=1}^M p_k(\lambda, m) q_m \tag{9}$$

with $p_k(\lambda, m)$ being the same function as in Eq. (7) but corresponding to a specific short-term environmental state with the number m.

The above presented $p_k(\lambda)$ functions are often regular in their tail, i.e. for extreme values of λ approaching extreme level 1. More precisely, for $\lambda \ge \lambda_0$, the distribution tail behaves like $\exp\{-(a\lambda + b)^c + d\}$ with a, b, c, d being fitted constants for appropriate tail cut-on λ_0 value. Optimal values of the parameters a, b, c, d may be determined using a sequential quadratic programming (SQP) technique implemented in NAG Numerical Library, (Numerical Algorithms Group, 2010).

GFX handles system as black box with infinite number of random parameters, as this method does not analyze any random parameters at all. Number of dimensions is also infinite, as all of them are simply merged into 1D vector $\boldsymbol{R}(t)$. The computational costs come mostly from FEM analysis, while statistical analysis comes at almost no costs (unless the vector $\boldsymbol{R}(t)$ size is very large).

In the next, ACER2D method is briefly introduced. Let $Z(t) = (X(t), Y(t))$ be a bivariate stochastic process, consisting of two synchronous scalar component processes $X(t), Y(t)$, that have been observed during some time interval $(0, T)$. In this paper it is assumed the sampled values $(X_1, Y_1), \ldots, (X_N, Y_N)$ are allocated at N equidistant discrete time instants $t_1, \ldots, t_N$ within $(0, T)$. The latter assumption however dos not limit proposed methodology, i.e. time sampling points can be reasonably non-equidistant. ACER2D aims at an accurate representation of the joint cumulative density function (CDF) of the extreme value vector $(\widehat{X}_N, \widehat{Y}_N)$, with $\widehat{X}_N = \max\{X_j; j = 1, \ldots, N\}$, and with a similar definition of $\widehat{Y}_N$. Thus, the aim is to get a robust estimate of the bivariate CDF function $P(\xi, \eta) := \text{Prob}\,(\widehat{X}_N \le \xi, \widehat{Y}_N \le \eta)$ for extreme values of ξ and η. In this paper ξ and η are the Jacket tubular support stresses.

The non-exceedance event is introduced $\mathscr{C}_{kj}(\xi, \eta) := \{X_{j-1} \le \xi, Y_{j-1} \le \eta, \ldots, X_{j-k+1} \le \xi, Y_{j-k+1} \le \eta\}$ for $1 \le k \le j \le N+1$. From the definition of CDF $P(\xi, \eta)$ it follows that

$$\begin{aligned}P(\xi, \eta) &= \text{Prob}\left(\mathscr{C}_{N+1,N+1}(\xi, \eta)\right)\\ &= \text{Prob}\left(X_N \le \xi, Y_N \le \eta \mid \mathscr{C}_{NN}(\xi, \eta)\right) \cdot \text{Prob}\left(\mathscr{C}_{NN}(\xi, \eta)\right)\\ &= \prod_{j=2}^N \text{Prob}\left(X_j \le \xi, Y_j \le \eta \mid \mathscr{C}_{jj}(\xi, \eta)\right) \cdot \text{Prob}\left(\mathscr{C}_{22}(\xi, \eta)\right)\end{aligned} \tag{10}$$

CDF distribution $P(\xi, \eta)$ can be expressed as

$$P(\xi, \eta) \approx \exp\left\{-\sum_{j=k}^N \left(\alpha_{kj}(\xi; \eta) + \beta_{kj}(\eta; \xi) - \gamma_{kj}(\xi, \eta)\right)\right\};\; \xi, \eta \to \infty \tag{11}$$

given that conditioning order parameter k is large enough. From Eq. (11) it is seen that estimation of the bivariate extreme value distribution requires accurate estimate of functions $\{(\alpha_{kj}(\xi; \eta) + \beta_{kj}(\xi; \eta) - \gamma_{kj}(\xi, \eta))\}_{j=k}^N$. Next, the k-th order bivariate average conditional exceedance rate (ACER) function is introduced

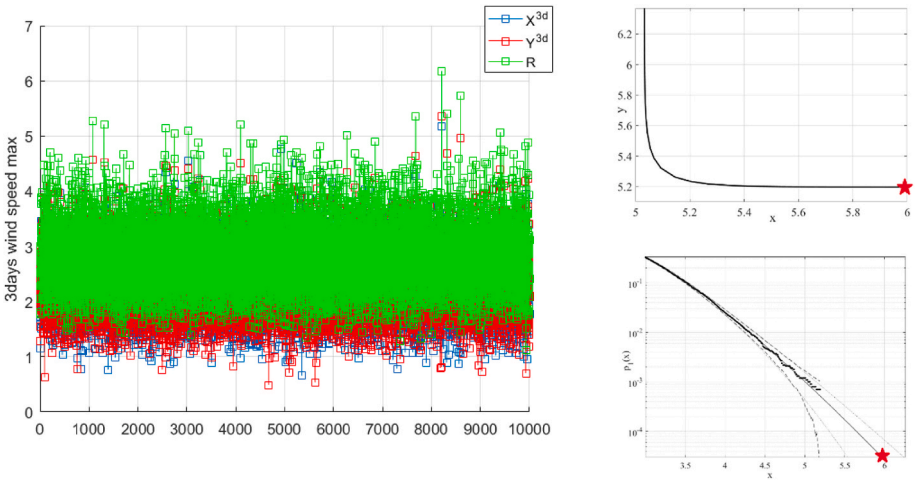

Fig. 4. Gumbel-Haugaard copula. Left: simulated time series. Right up: corresponding ACER2D bivariate contour, Right low: GFX prediction for $\vec{R}$ vector.

$$\mathscr{E}_k(\xi,\eta)=\frac{1}{N-k+1}\sum_{j=k}^{N}\left(\alpha_{kj}(\xi;\eta)+\beta_{kj}(\eta;\xi)-\gamma_{kj}(\xi,\eta)\right), k=1,2,\ldots \tag{12}$$

Therefore, when $N\gg k$, one may write

$$P(\xi,\eta)\approx\exp\{-(N-k+1)\ \mathscr{E}_k(\xi,\eta)\}\ ;\ \ \xi,\eta\to\infty \tag{13}$$

Numerical estimation of the bivariate ACER function for the observed stationary series consists in counting of the appropriate exceedance events, with $\mathscr{E}_k(\xi,\eta,m)$ being the ACER function (13), estimated for a particular stationary sea state, for numerical implementation see (https://github.com/gocrane/crane). According to Eq. (13), which is a definition of the bivariate ACER function $\mathscr{E}_k(\xi,\eta)$, the product $(N-k+1)\cdot\mathscr{E}_k(\xi,\eta)$ is equal to expected number of bivariate observations $Z_j=(X_j,Y_j)$ such that their components exceed one of two corresponding response levels ξ and η (not necessary simultaneously), and which follow after at least $k-1$ immediately preceding simultaneous non-exceedances. Thus the bivariate ACER function $\mathscr{E}_k(\xi,\eta)$ captures dependence structure between components X_j and Y_j of underlying bivariate time series. For a pair of random variables (X,Y) with marginal CDFs $F_x(\xi)$ and $G_y(\eta)$, the joint CDF $H_{xy}(\xi,\eta)=\text{Prob}\ (X\le\xi,Y\le\eta)$ can be represented as bivariate copula $C(u,v)$; the latter copula in this paper is chosen to be either Gumbel logistic (GL) or the Asymmetric logistic (AL) see (Gaidai et al., 2022d). Assuming that the marginal extreme value CDFs are presented through the corresponding univariate ACER functions

$$\begin{aligned} F_x(\xi) &\approx\exp\{-(N-k+1)\varepsilon_k^x(\xi)\}\ ,\xi\ge\xi_1\\ G_y(\eta) &\approx\exp\{-(N-k+1)\varepsilon_k^y(\eta)\}\ ,\eta\ge\eta_1\end{aligned} \tag{14}$$

where $\varepsilon_k^x(\xi)=q_k^x\exp\{-a_k^x(\xi-b_k^x)^{c_k^x}\}$ with a similar definition of $\varepsilon_k^y(\eta)$. For the details on optimization procedure for estimation of $a_k^x,b_k^x,c_k^x,q_k^x,a_k^y,b_k^y,c_k^y,q_k^y$ see (Xu et al., 2022a).

3. Synthetic example

In this section authors have deliberately selected synthetic example, as exact analytical solutions for underlying probability distributions are known in advance. That will allow not only to compare statistical methods, but cross-validate them versus exact predictions. Wind speeds prediction is an important engineering research topic (Thoft-Christensen and Murotsu, 1986),- (Leimeister and Kolios, 2021).

Let one consider 3.65-day maximum wind speed process $X(t)$ simulated during the given time interval $[0,T]$. The underlying normalized non-dimensional stochastic processes $U(t)$ has been modelled as a stationary Gaussian process with zero mean value and a standard deviation equal to one. Therefore it was assumed that the $U(t)$ mean zero upcrossing rate satisfies the equality $\nu_U^+(0)=10^3/T$, with $T=1$ year, the latter assumption is common in offshore wind engineering.

For this numerical example, the data record had been chosen to contain 10^4 data points, which is equivalent to 100 years record, since wind speed maxima process $X(t)$ has $365/3.65=10^2$ data points per year.

The underlying wind speed process $U(t)$ results in 3.65 days maximum analytical CDF distribution $F_X^{3d}(x)=\exp\left\{-q\exp\left(-\frac{x^2}{2}\right)\right\}$ for the wind speed three days maxima process $X^{3d}(t)$, with $q=10$, see (Naess and Moan, 2013) for details. There are three Archimedian copulas in common use: Clayton, Frank and Gumbel-Haugaard.

First, the Gumbel-Haugaard copula dependence structure $G(u,v)$ between the two marginal peak wind speed variables $X^{3d}(t)$ and identically distributed correlated process $Y^{3d}(t)$ is considered:

$$G(u,v)=\exp\left\{-\left[(-\log u)^m+(-\log v)^m\right]^{\frac{1}{m}}\right\} \tag{15}$$

with parameter $m=1/\sqrt{1-R_{corr}}$ being related to the correlation coefficient R_{corr} between two processes $X^{3d}(t)$ and $Y^{3d}(t)$; in this section R_{corr} was set to 0.5 for simplicity. As the underlying wind speed processes $X(t)$, $Y(t)$ are identically distributed stationary Gaussian processes, and Gumbel-Haugaard copula is quite easy to fit for ACER2D method, it is expected that it will be no significant difference between GFX and ACER2D predictions in terms of predicted decimal logarithm probability level for a given response level (wind speed in this case) of interest. For this section following response levels have been chosen: $x=6,y=5.2$.

The bivariate extreme value distribution of the peak event data was

$$H^{3d}(x,y)=\exp\left\{-\left[q\exp\left(-m\frac{x^2}{2}\right)+q\exp\left(-m\frac{y^2}{2}\right)\right]^{\frac{1}{m}}\right\} \tag{16}$$

Fig. 4 presents simulated time series, along with corresponding ACER2D bivariate contour and GFX prediction for $\vec{R}$ vector, red star indicated target probability level. As expected agreement between both methods was very good.

Second, the Clayton copula $C(u,v)$ being an asymmetric Archimedean copula was applied in analogous way instead of Gumbel-Haugaard copula.

$$C(u,v)=\max\left\{\left[u^{-m}+v^{-m}\right]^{-\frac{1}{m}},0\right\} \tag{17}$$

Clayton copula is less convenient to fit by ACER2D as it is not in its copula library, therefore in this case ACER2D is expected to perform less accurate than GFX method, as obviously GFX does not have copula

Fig. 5. An example of offshore Jacket platform operating in the Bohai continental shelf.

approximation assumption. All numerical parameters have been unchanged with respect to the previous Gumbel-Haugaard copula case. By performing a series of independent synthetic tests it was found that indeed GFX method predicts exceedance probability decimal logarithm level more accurate than ACER2D. For numerical set up as described above it was found that on average GFX performs about 15% more accurate than ACER2D. Note however that synthetic data was based on underlying Gaussian process and Archimedian copulas, predicted level chosen was not that extreme, and in case of real measured non-Gaussian, cross-correlated by non-Archimedian copula data, the GFX advantage may be much more pronounced. Last but not least, computational effort of ACER2D is of course much bigger that GFX method for any given bivariate failure limit, as ACER2D performs two-dimensional surface interpolation; the latter is particularly important when analyzing large data sets like in the next section.

4. Jacket and environmental conditions modelling

Offshore Jackets have been studied by many researchers for quite a long time (Song, 2017),- (Skjelbreia and Hendrickson, 1961). Fig. 5 presents an example of Jacket platform, similar to the one studied here. Offshore Jacket was modelled as a multi-degree of freedom 4D structure using ANSYS finite element (FEM) software.

The ANSYS FEM software is used to simulate response time histories. Jacket dynamic model is based on the assumption that the hydrodynamic forces acting on the structure are distributed over discrete nodes, located from the deck structure to the sea bottom. This is reasonable assumption, since wave height is not large enough to cause wave in deck jolt. The lumped parameter model can be expressed in the following vector form $M\ddot{X} + C\dot{X} + KX = F_{in} + F_d$ with M, C and K are constant matrices (geometric non-linearity is not modelled). Morison drag force is given in the relative velocity formulation, therefore non-linearity enters model though the right hand side of dynamic equation, namely through the Morison drag force.

Response vector $X = (x_1, ..., x_N)^T$ consists of components$x_k = x_k(t)$, $k = 1..., N$, being the k-th degree of freedom (DOF); N is the number DOFs in FEM model. F_{in} and F_d are inertia and drag force components respectively. For more information about the Morison equation (Sumer and Fredsøe, 1997). The inertial force F_{in} can be expressed as $F_{in} = \rho C_m A(\dot{X}_w - \dot{X}) + \rho A\dot{X}_w$ where ρ denotes the water density, C_m denotes the hydrodynamic-mass coefficient, A denotes the cross-sectional area of the body, $\dot{X}_w$ is the velocity of the water particle due to waves and currents. $\rho C_m A(\dot{X}_w - \dot{X})$ is the hydrodynamic mass force, while $\rho A\dot{X}_w$ is the Froude-Krylov force. The drag force $\boldsymbol{F}_d$ can be expressed as $F_d = \frac{1}{2}\rho C_D D(\dot{X}_w - \dot{X})|\dot{X}_w - \dot{X}|$ where C_D is the drag coefficient, D is the cylinder diameter. The velocity of the water particle is calculated by the wave and current settings, i.e. wave direction, wave theory, wave height, wave period, current direction, current speed, etc. They will be discussed in the next section.

The Newmark-β method is applied to solve the nonlinear dynamic equation. If the algorithm parameters are properly chosen, the Newmark-β method can be stable unconditionally.

Satellite based global wave statistics was used to obtain proper wave

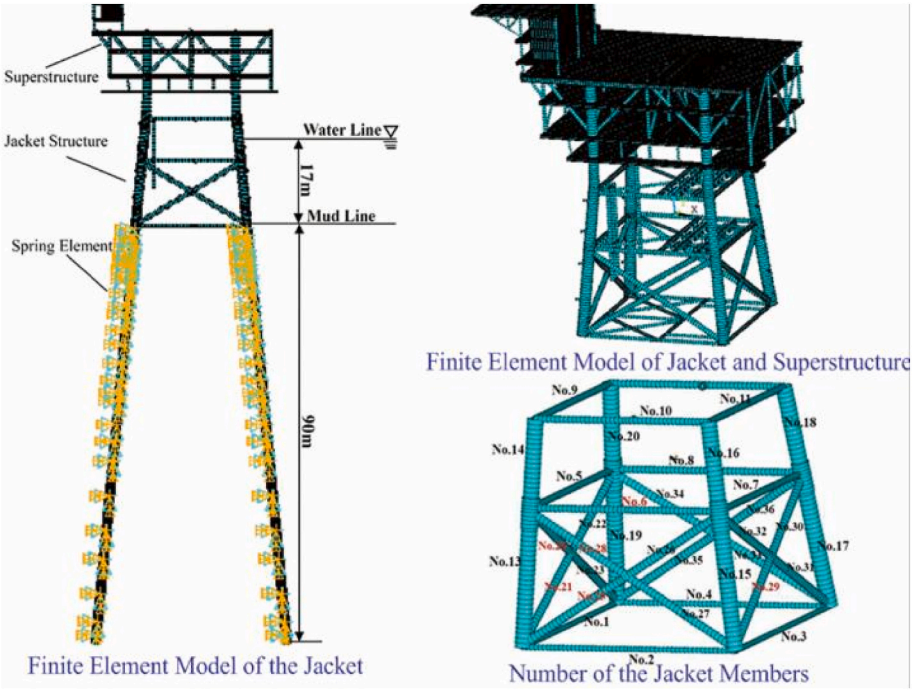

Fig. 6. Finite element model of the Jacket.

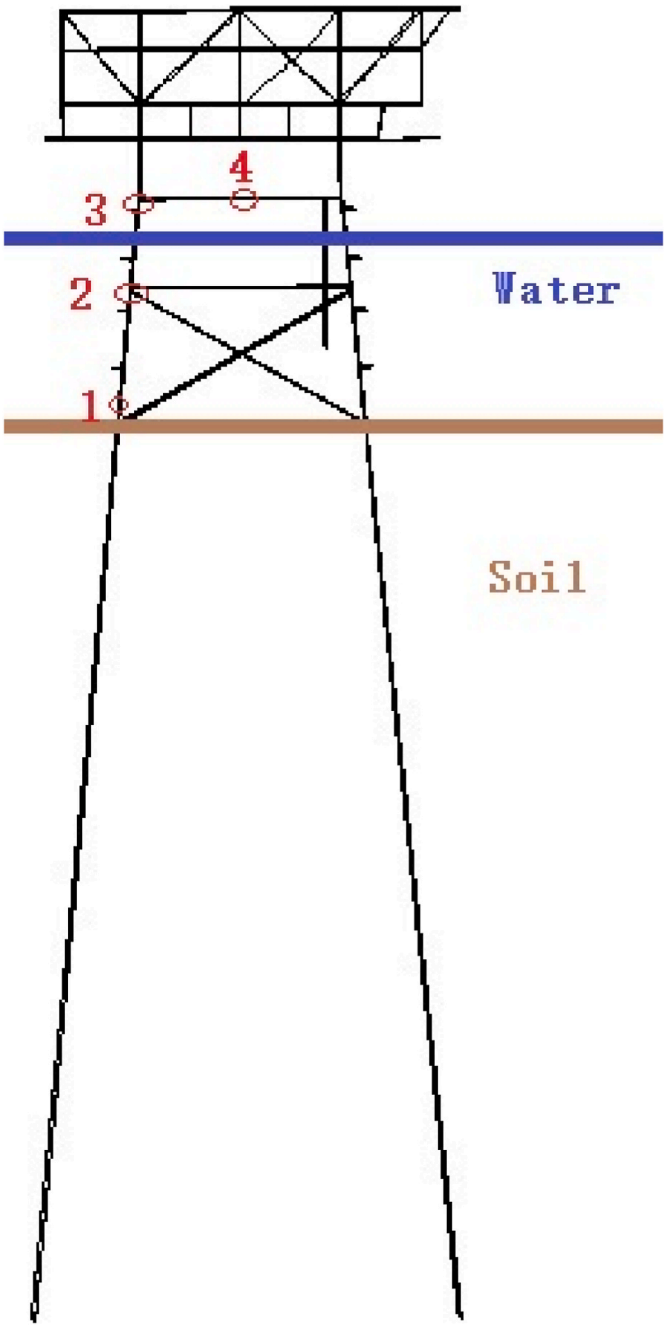

Fig. 7. Schematic Jacket illustration with four stress monitoring location spots.

scatter diagram for the Bohai bay area. Specifically, the Global Wave Statistics Online (http://www.globalwavestatisticsonline.com/) data was utilized. Fig. 1 presents annually averaged spatial distribution of wave height along with wave period in Bohai bay area of interest, star indicates Jacket location. A 3-h stationary storm simulation was run for each sea state. Stationary sea state was specified according to the JONSWAP wave spectrum, namely given by the one-sided power spectral density (PSD) of the wave elevation $\eta(t)$ denoted by $S_{\eta}^{+}(\omega)$, $\omega > 0$, as follows

$$S_{\eta}^{+}(\omega) = \frac{\alpha g^2}{\omega^5} \exp\left\{ -\frac{5}{4}\left(\frac{\omega_p}{\omega}\right)^4 + \ln\gamma \exp\left[-\frac{1}{2\sigma^2}\left(\frac{\omega}{\omega_p} - 1\right)^2 \right] \right\} \tag{18}$$

with $g = 9.81$ m/s^2, ω_p is the peak frequency in rad/s; α, γ and σ are parameters related to the spectral shape; $\sigma = 0.07$ when $\omega \leq \omega_p$, $\sigma =$ 0.09 when $\omega > \omega_p$. For Bohai bay the parameter γ is chosen to be 3.3, see (DNV-RP-C205, 2010; DNV-RP-H103, 2011).

The parameter α was determined from equation $\alpha = 5.06\left(\frac{H_s}{T_p^2}\right)^2 (1 - 0.287 \ln\gamma)$; with H_s being significant wave height, and $T_p = 2\pi/\omega_p$ being spectral peak wave period.

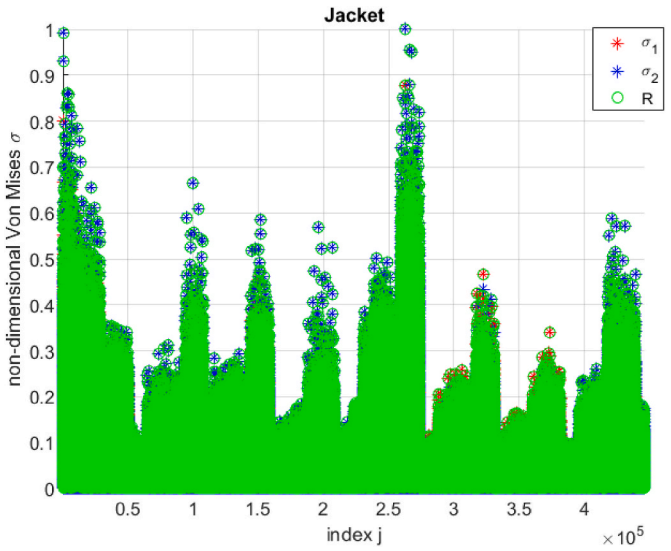

Fig. 8. Example of von Mises Jacket stresses with subtracted mean. Non-dimensional, presented as time series.

5. Jacket model

Jacket was modelled as a multi-degree of freedom (MDOF) 4D structure using ANSYS finite element software (FEM). Fig. 6 depicts investigated Jacket platform operating on the Bohai Continental Shelf.

6. Reliability study results for structural support stresses

This section presents statistical results, corresponding to the two selected Jacket tubular support member stresses. Since simulation was performed synchronously for the whole Jacket platform structure.

Fig. 7 presents schematic Jacket illustration with four stress monitoring location spots.

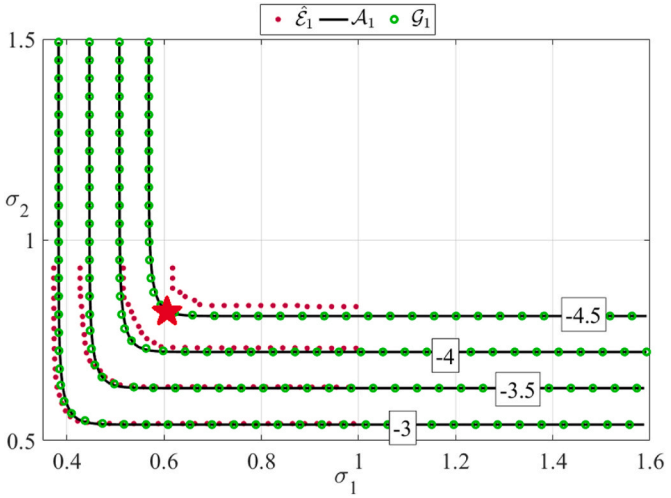

Fig. 9. ACER2D bivariate contours for Jacket non-dimensional stresses.

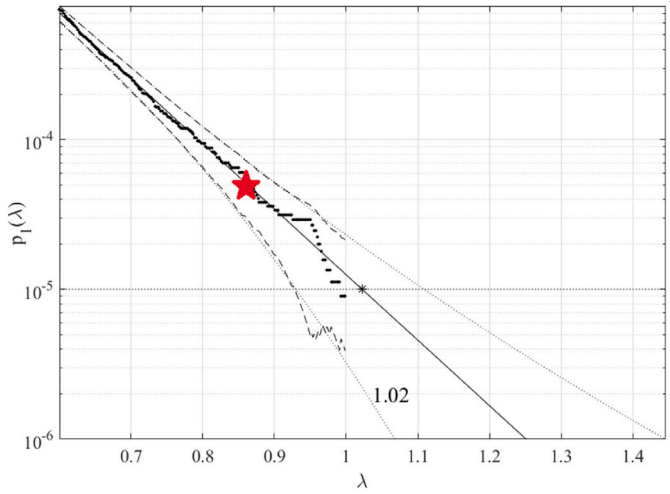

Fig. 10. GFX prediction. Star indicates the same bivariate failure level of interest.

7. Method validation

This section illustrates efficiency of GFX method, by means of application to Jacket stresses data set. Two different Jacket stresses located at number 1 and 2 points indicated in Fig. 7 were chosen as components X, Y thus constituting an example of two dimensional (2D) dynamic system.

Unidimensional extreme response values roughly corresponding to 5 years return period where taken as critical thresholds, chosen Jacket components to fail.

In order to unify all three measured time series X, Y the following scaling was performed according Eq. (11) making both two responses non-dimensional and having the same failure limit equal to 1. Next, all local maxima from three measured time series were merged into one single time series by keeping them in time non-decreasing order: $\vec{R} = (\max\{X_1, Y_1\}, \ldots, \max\{X_N, Y_N\})$. In order to unify all three measured time series X, Y the following scaling was performed

$$X \to \frac{X}{\eta_X}, Y \to \frac{Y}{\eta_Y} \tag{19}$$

Fig. 8 presents example of von Mises Jacket stresses with subtracted mean value for different sea states, both dimensional and non-dimensional stresses.

Fig. 9 presents ACER2D bivariate contours for Jacket stresses. It is seen from Fig. 9 that ACER2D fits different Gumbel copula to the measured data, and there is an inherent error due to particular copula choice. Fig. 10 presents GFX prediction, with star indicating the same bivariate failure level of interest. Note that both Figs. 9 and 10 exhibit certain agreement for the target probability level p, indicated by star. For more details on ACER2D method see (Xu et al., 2022a, 2022b; Gaidai et al., 2022b, 2022c, 2022d). For more details on GFX method see (Gaidai et al., 2022). Bivariate non-dimensional failure point $\eta_X = 0.6$, $\eta_Y = 0.84$ was chosen above because in lies on 5 years contour line, estimated by ACER2D. The probability level p corresponding to this contour line was then compared with GFX method estimate. It was found that ACER2D probability level estimate lied well within 95% CI (Confidence Interval), predicted by GFX method. For numerical code behind GFX extrapolation, see GitHub repository. (https://github.com/gocrane/crane).

8. Conclusions

Classic reliability methods, dealing with time series do not have an advantage of dealing efficiently with systems possessing high dimensionality and cross-correlation between different system responses. The key advantage of the introduced methodology is its ability to study reliability of high dimensional dynamic systems.

This paper studied both synthetic wind speed data set as well as simulated Jacket dynamic response time series measured in few critical structural locations. Theoretical reasoning behind the proposed method is given in detail. Note that use of direct either measurement or Monte Carlo simulation for dynamic system reliability analysis is attractive, however dynamic system complexity and its high dimensionality require development of novel robust and accurate techniques that are able to deal with a limited data set at hand, utilizing available data as efficient as possible.

The method introduced in this paper, has been previously validated by application to a wide range of simulation models, but for only one-dimensional system responses and, in general, very accurate predictions were obtained. This study aimed at further development of a general purpose, yet robust and simple to use multi-dimensional reliability method.

Novel method was validated versus ACER2D bivariate method using both analytical synthetic data.

Finally, the suggested methodology can be used in wide range of engineering areas of applications. The presented naval architecture example does not limit areas of new method applicability by any means.

Novelty and contribution

- A novel health system reliability method has been developed and applied to the real engineering data set
- Novel method has been validated versus existing one
- Proper confidence bands may be given

CRediT authorship contribution statement

Oleg Gaidai: Conceptualization, Data curation, Formal analysis, Investigation, Methodology, Project administration. **Yihan Xing:** Resources, Software, Supervision, Validation, Visualization, Writing – original draft.

Declaration of competing interest

The authors declare that they have no known competing financial interests or personal relationships that could have appeared to influence the work reported in this paper.

Data availability

Data will be made available on request.

Acknowledgements

Authors declare no conflict of interests. No funding was received. All authors contributed equally. The authors would like to thank the owner, manager, superintendents, masters and crew for their assistance in obtaining the measurement data. Further thanks to DNV for support and sharing measurement data for this research.

References

Adcock, T.A.A., Draper, S., 2015. The second order contribution to wave crest amplitude - random simulations and new wave. In: Proceedings of the 25th International Offshore and Polar Engineering Conference, pp. 488–493.

DNV-RP-C205, 2010. Environmental Conditions and Environmental Loads.

DNV-RP-H103, 2011. Modelling and Analysis of Marine Operations.

Gaidai, O., Fu, S., Xing, Y., 2022. Novel reliability method for multidimensional nonlinear dynamic systems. Mar. Struct. 86 https://doi.org/10.1016/j.marstruc.2022.103278.

Gaidai, O., Wang, F., Wu, Y., Xing, Y., Medina, A., Wang, J., 2022a. Offshore renewable energy site correlated wind-wave statistics. Probabilist. Eng. Mech. 68 https://doi.org/10.1016/j.probengmech.2022.103207.

Gaidai, O., Xing, Y., Wang, F., Wang, S., Yan, P., Naess, A., 2022b. Improving extreme anchor tension prediction of a 10-MW floating semi-submersible type wind turbine, using highly correlated surge motion record. Front. Mech. Eng. 51 https://doi.org/10.3389/fmech.2022.888497.

Gaidai, O., Xing, Y., Xu, X., 2022c. COVID-19 epidemic forecast in USA East coast by novel reliability approach. Research square. https://doi.org/10.21203/rs.3.rs-1573862/v1.

Gaidai, O., Xing, Y., Balakrishna, R., 2022d. Improving extreme response prediction of a subsea shuttle tanker hovering in ocean current using an alternative highly correlated response signal. Results in Engineering. https://doi.org/10.1016/j.rineng.2022.100593.

http://www.globalwavestatisticsonline.com/.

https://github.com/gocrane/crane.

Leimeister, M., Kolios, A., 2021. Reliability-based design optimization of a spar-type floating offshore wind turbine support structure. Reliab. Eng. Syst. Saf. 213 https://doi.org/10.1016/j.ress.2021.107666.

Lv, X., Yuan, D., Ma, X., Tao, J., 2014. Wave characteristics analysis in Bohai Sea based on ECMWF wind field. Ocean Eng. 91, 159–171.

Melchers, R.E., 1999. Structural Reliability Analysis and Prediction. John Wiley & Sons, Inc, New York.

Naess, A., Moan, T., 2013. Stochastic Dynamics of Marine Structures. Cambridge University Press.

Naess, A., Leira, B.J., Batsevych, O., 2009. System reliability analysis by enhanced Monte Carlo simulation. Struct. Saf. 31, 349–355.

Naess, A., Leira, B.J., Batsevych, O., 2012. Reliability analysis of large structural systems. Probabilist. Eng. Mech. 28, 164–168.

Norwegian Meteorological Institute. https://seklima.met.no/.

Numerical Algorithms Group, 2010. NAG Toolbox for Matlab. NAG Ltd, Oxford, UK.

Rice, S.O., 1944. Mathematical analysis of random noise. Bell System Tech. J. 23, 282–332.

Sharma, J., Dean, R.G., 1981. Second-order directional seas and associated wave forces. J. Soc. of Petr. Eng. 129–140. SPE.

Skjelbreia, L., Hendrickson, J.A., 1961. Fifth order gravity wave theory. In: Proceedings, Seventh Conference on Coastal Engineering, vol. 10, pp. 184–196.

Song, Z., 2017. Reliability evaluation of jacket-type offshore platforms subjected to wind, wave, and current loads. In: IOP Conference Series Earth and Environmental Science, vol. 86. https://doi.org/10.1088/1755-1315/86/1/012009, 1.

Sumer, B., Fredsøe, J., 1997. Hydrodynamics Around Cylindrical Structures", vol. 12. World Scientific.

Sun, J., Gaidai, O., Wang, F., Naess, A., Wu, Y., Xing, Y., van Loon, E., Medina, A., Wang, J., 2022a. Extreme riser experimental loads caused by sea currents in the Gulf of Eilat. Probabilist. Eng. Mech. 68 https://doi.org/10.1016/j.probengmech.2022.103243.

Sun, J., Gaidai, O., Wang, F., Naess, A., Wu, Y., Xing, Y., van Loon, E., Medina, A., Wang, J., 2022b. Extreme riser experimental loads caused by sea currents in the Gulf of Eilat. Probabilist. Eng. Mech. 68 https://doi.org/10.1016/j.probengmech.2022.103243.

Thoft-Christensen, P., Murotsu, Y., 1986. Application of Structural Systems Reliability Theory. Springer-Verlag, Berlin.

Wang, Z., Wu, K., Zhou, L., Wu, L., 2012. Wave characteristics and extreme parameters in the Bohai sea. China Ocean Eng. 26 (2), 341–350.

Xing, Y., Gaidai, O., Ma, Y., Naess, A., Wang, F., 2022. A novel design approach for estimation of extreme responses of a subsea shuttle tanker hovering in ocean current considering aft thruster failure. Appl. Ocean Res. 123 https://doi.org/10.1016/j.apor.2022.103179.

Xu, X., Wang, F., Gaidai, O., Naess, A., Xing, Y., Wang, J., 2022a. Bivariate statistics of floating offshore wind turbine dynamic response under operational conditions. Ocean Eng. 257 https://doi.org/10.1016/j.oceaneng.2022.111657.

Xu, X., Xing, Y., Gaidai, O., Wang, K., Sandipkumar Patel, K., Dou, P., Zhang, Z., 2022b. A novel multi-dimensional reliability approach for floating wind turbines under power production conditions. Front. Mar. Sci. https://doi.org/10.3389/fmars.2022.970081.

Zhao, Y.G., Ono, T., 1999. A general procedure for first/second order reliability method (FORM/SORM). Struct. Saf. 21 (2), 95–112.